



US Army Corps
of Engineers®

Deep-Draft Entrance Channels: Preliminary Comparisons Between Field and Laboratory Measurements

*by Michael J. Briggs, Ivano Melito,
Zeki Demirbilek, and Frank Sargent*

PURPOSE: This Coastal and Hydraulics Engineering Technical Note (CHETN) summarizes preliminary comparisons between field and laboratory measurements of wave-induced vertical motions at Barbers Point Harbor, HI (Figure 1). The importance of these wave motions to ship underkeel clearance allowances and channel depth requirements is described.



Figure 1. Aerial view of Barbers Point Harbor, HI

NEEDS AND BENEFITS: The next generation of ships will require deeper and wider entrance channels to provide safe navigation. Channel width and depth depend on vessel size, traffic flow, and environmental conditions such as tides, water levels, winds, waves, and currents. Channel depth is determined by ship draft and trim (T), and gross underkeel clearance allowances (h_{UKC}). The h_{UKC} is composed of several factors including (a) tides (h_{TI}), (b) wave-induced motions (h_{WA}), (c) squat (h_{SQ}), and (d) a safety factor for seabed type (h_{SF}). Additional clearances can also be included for dredging tolerance and advance maintenance (h_{AM}). Squat is a drawdown of the ship due to decreased pressure beneath the hull as it moves ahead at nearly constant speed in shallow and confined seaways. Wider and deeper channels require project and maintenance dredging, with costs of the order of \$150,000 per vertical foot per acre, depending on the type of seabed. The U.S. Army Corps of Engineers spends over \$500 million per year

(approximately one-third of the Corps O&M budget) on dredging. Thus, the dilemma is to minimize the h_{UKC} and corresponding costs while still ensuring safe navigation.

Available guidance for predicting h_{UKC} is inadequate as there is little field and laboratory data or numerical models to improve and validate this guidance. For the h_{WA} component, EM 1110-2-1613 (HQUSACE 1995) recommends a value equal to 1.2 times the incident wave height H_I , whereas the Permanent International Association of Navigation Congresses (1997) recommends a value up to 0.4 times the ships' draft T . Typical harbors operate with $1.2 \text{ m (4 ft)} \leq h_{WA} \leq 2.4 \text{ m (8 ft)}$, regardless of ship draft and wave height. Individual states have their own guidelines that may differ substantially from each other. For example, the Hawaii Department of Transportation recommends a h_{UKC} of 1.8 m (6 ft) in the entrance channel, compared to 2.4 m (8 ft) by the Corps. This 0.6-m (2-ft) difference significantly increases the cost of project and maintenance dredging.

Realistic and accurate measurement of vessel motions in prototype and at laboratory scales is critical to developing improved deep-draft design guidance. Prototype ship motions and environmental data were obtained in the unconfined entrance channel at Barbers Point Harbor, HI in May 1999 for five ships. These field measurements were reproduced in a controlled laboratory study of Barbers Point Harbor for one of the ships. The purpose of this CHETN is to document comparisons between the laboratory and field measurements of wave-induced vertical ship motions and define any scale effects that may exist. Good comparisons will validate the physical model as a predictive tool for these vertical ship motions and, more importantly, h_{UKC} .

The goal of this research is to develop data to improve the U.S. Army Engineer Research and Development Center (ERDC) ship simulator and provide an empirical approach to aid in coastal entrance channel design. Limited field and laboratory measurements of wave-induced, vertical ship motions have been made at Barbers Point. Deterministic design curves will be provided from these empirical data. Ultimately, a probabilistic model for predicting the total underkeel clearance allowance h_{UKC} that includes h_{WA} , h_{TI} , and h_{SQ} must be developed to account for the random nature of ship transits in entrance channels. Borgman (2001) has proposed a novel approach for dealing with the statistics from this laboratory data that can extend their use for different ships.

FIELD STUDY

Barbers Point Harbor: The Barbers Point Harbor is located on the southwest coastline of Oahu (Figure 1) and consists of a deep-draft harbor, barge basin, resort marina, and entrance channel (Briggs et al. 1994). The deep-draft harbor has an area of 0.364 km^2 (90 acres) and is 11.6 m (38 ft) deep. A harbor extension was added in 1998. The barge basin is 67.1 m (220 ft) by 396.2 m (1,300 ft) and 7.0 m (23 ft) deep. The West Beach Marina has a depth of 4.6 m (15 ft) and was designed to accommodate 350 to 500 small boats. The entrance channel is 137.2 m (450 ft) wide, 1158.2 m (3,800 ft) long, and 12.8 m (42 ft) deep. It has a trench cross-section, with sloping sides that intersect the existing bathymetry along its length. Stations were located every 30.5 m (100 ft) along the channel for ship positioning. Sta 0 is located at the offshore end of the channel, approximately 243.8 m (800 ft) from the 100-ft (30.5-m) depth

contour. The harbor regularly services barges, tankers, and bulk carriers. Bulk carriers make approximately 120 transits per year.

Prototype Measurements: In May 1999, a Differential Global Positioning System (DGPS) was used to record six degree-of-freedom (DOF) vessel motions on five different vessels transiting the entrance channel at Barbers Point. Table 1 lists design vessel parameters for these five vessels from the vessel owners. Two of the vessels were bulk carriers and three were oil tankers. All vessels had bulbous bows except for the *Igrim*, which is a smaller icebreaker tanker. The *World Utility* is typical of the vessel size and shape for the bulk carriers (Figure 2). Table 2 summarizes the transit parameters for the five vessels including dates, times, ship loading condition, and actual drafts for inbound and outbound runs. Ship loading reflects the fact that the ships were not fully loaded for all transits. Three of the vessels were fully-loaded on the inbound leg and two on the outbound leg. The actual drafts reflect the vessel trim at the bow and stern during these field measurements and are slightly different than the design or full-load drafts shown in Table 1.

Table 1 Vessel Parameters Barbers Point Harbor, HI								
Vessel		Type	LOA, m	Beam, m	Full Load Draft, m	Displacement, mt		Block Coef.
Name	Code					Full-Load	Light Ship	
<i>Atoyac</i>	A	Bulk Carrier	185.7	30.4	11.6	53,181	7,539	0.83
<i>Carla A. Hills</i>	CAH	Oil Tanker	179.2	30.4	11.0	45,257	N/A	0.79
<i>Igrim</i>	I	Oil Tanker	160.0	23.0	9.4	24,964	7,564	N/A
<i>Port Catherine</i>	PC	Oil Tanker	180.0	32.2	11.2	54,613	9,690	N/A
<i>World Utility</i>	WU	Bulk Carrier	196.1	32.2	11.7	57,544	9,715	0.76

Notes:
N/A = Not Available for the ship



Figure 2. *World Utility* bulk cargo carrier

Table 2 Transit Parameters Barbers Point Harbor, HI													
Vessel		Inbound Runs						Outbound Runs					
Name	Code	Date	Time	Tide, m	Load	Draft, m		Date	Time	Tide, m	Load	Draft, m	
						Bow	Stern					Bow	Stern
<i>Atoyac</i>	A	21	6:30	+0.2	F	8.92	10.12	25	6:30	+0.0	L	4.36	6.85
<i>Carla A. Hills</i>	CAH	18	9:00	+0.0	L	4.47	7.54	19	18:30	+0.6	F	7.39	8.96
<i>Igrim</i>	I	5	11:00	+0.0	F	7.90	10.10	9	9:00	+0.2	L	7.40	9.50
<i>Port Catherine</i>	PC	14	12:00	+0.2	F	9.70	9.70	16	12:00	+0.7	L	5.55	7.70
<i>World Utility</i>	WU	20	6:30	+0.2	L	4.29	6.43	30	10:00	+0.2	F	10.75	10.92

Notes:
 1. Date is relative to May 1999
 2. Time is Hawaii Standard Time (HST)
 3. F = Full load (MAX draft), L = Light load (MIN draft)

Three GPS sensors were positioned on each vessel, two on either side of the bridge and one at the bow of these vessels. The bow sensor was located several feet from the bow on the longitudinal center line and the port and starboard sensors were located on both sides of the bridge wings, approximately 30.5 m (100 ft) forward of the stern. A land-based GPS receiver was used in this dual-frequency, DGPS system to insure cm-level accuracy of the measurements. All GPS data were referenced to a static ship survey. Engine speed and rudder commands were also recorded.

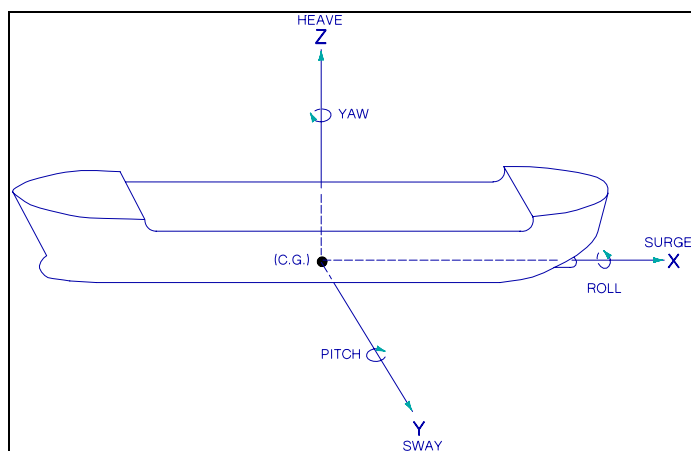


Figure 3. The 6-deg of freedom ship motions

The six DOF motions of a moving ship are the three translations of surge, sway, heave, and the three rotations of roll, pitch, and yaw (Figure 3). A ship typically rotates about the center of gravity (CG), located on the longitudinal center line approximately amidships. The wave-induced portion of the h_{UKC} is a function of the vertical motions from heave, pitch, and roll.

The vertical motions from the three GPS sensors were averaged to obtain the net vertical excursion for each

ship transit. The location of the average of the three sensors is approximately equal to the CG. A digital filter was applied to the data with a cutoff of 30 sec to separate low and high frequency components. The low frequency portion corresponds to the vessel squat and the high frequency to the wave-induced vertical motions. Measured squat was less than 1 ft (0.30 m), and very transient due to the short channel and varying ship speeds.

Wave Conditions: Environmental data were collected at 1 Hz for 20 min every 3 hr using a PUV pressure gage located in the entrance channel and a National Oceanic and Atmospheric Administration (NOAA) buoy located approximately 363 km (196 navigation mile (NM)) from the site. The pressure gage was positioned approximately 0.9 m (3 ft) off the bottom and 1.5 m (5 ft) from the south channel wall near Sta 2200. Figure 4 is a time series of wave heights measured for both the pressure and NOAA buoy. Offshore wave heights varied from 1.2 to 2.7 m (4 to 9 ft), while inshore values were between 0.3 to 0.6 m (1 to 2 ft). In general, pressure gage data collection was continuous and good quality with missing data only from 28 to 31 May. Large offshore wave heights at the buoy do not necessarily correspond to larger wave heights in the channel because of directional characteristics of the waves and nearshore processes such as bathymetry, diffraction, reflection, and wave breaking that may strongly affect wave energy inside the channel. Directional wave data were measured in the channel with the PUV gage, but preliminary analysis indicated that the directional analysis was not reliable due to the wave transformation inside the entrance channel. Visual observations during ship transits, however, indicated that waves were primarily from the south with some spreading.

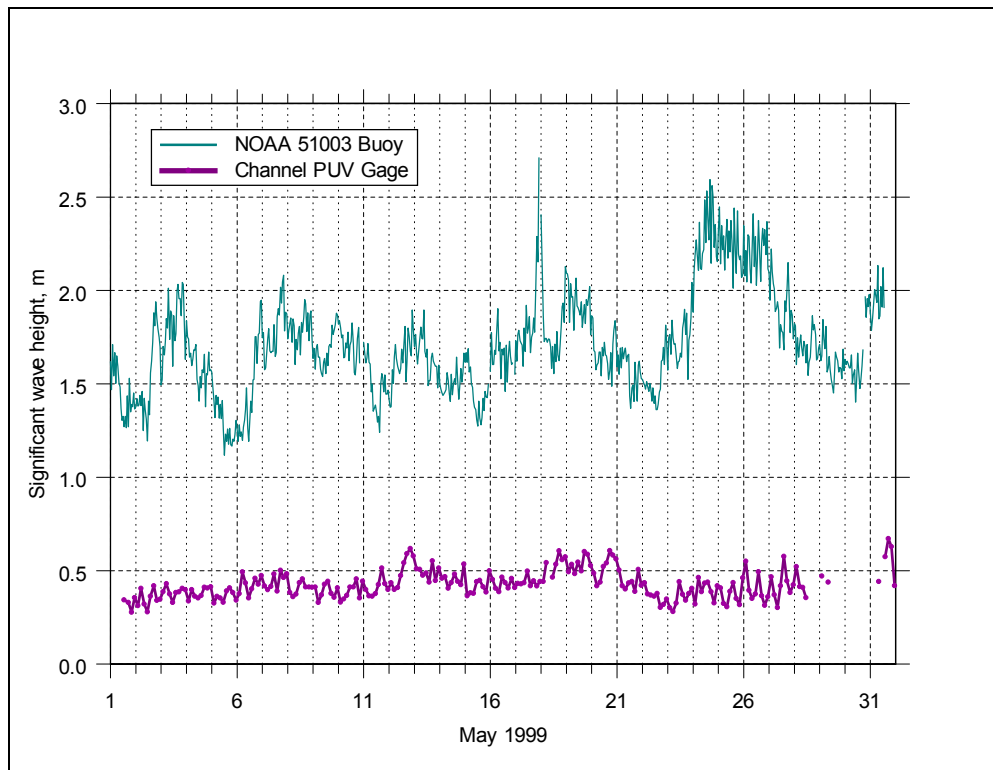


Figure 4. Measured significant wave heights by the NOAA offshore buoy and the entrance channel PUV gage

PHYSICAL MODEL STUDY

Model Setup: An undistorted, three-dimensional model of Barbers Point Harbor (Figure 5) was constructed in 1990 at a model to prototype scale $L_r = 1:75$ (Briggs et al. 1994). The near-shore area extends to the 30.5-m (100-ft) mllw contour and includes approximately 1,067 m² (3,500 ft²) on either side of the entrance channel. Total area of the model is over 1,022 m²

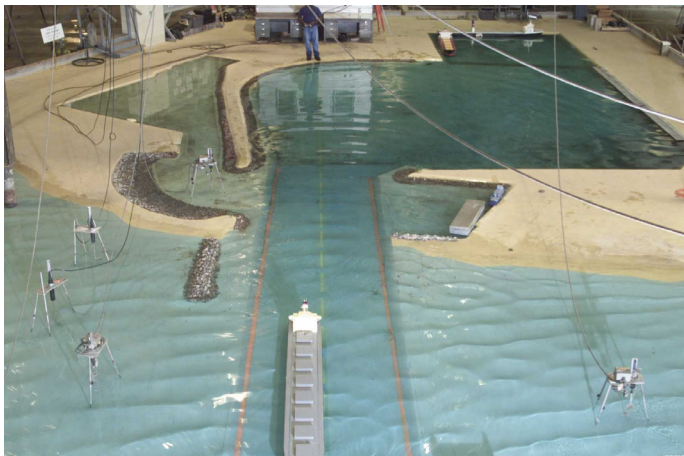


Figure 5. Physical model of Barbers Point Harbor at the ERDC, Coastal and Hydraulics Laboratory (CHL) research facilities

(11,000 ft²). The model scale was selected to allow proper reproduction of hydrodynamic conditions.

Model Ship: A 1:75 scale model of the *World Utility* was used in this study because its shape and dimensions are typical of the cargo carriers and tankers using the harbor during the prototype measurements (Figure 6). The ship has a length of 196 m (643 ft), a beam of 32 m (105 ft), a draft of 10.9 m (35.8 ft) at a full-load displacement of 57,500 metric tons (mt) (1 mt = 1,000 kg), and a draft of 6.5 m (21.3 ft) at a light ship displacement

of 9,700 mt (see Table 2). Forward and reverse speeds and rudder angle were remote-controlled. The vessel was statically balanced with measured weight distribution and a digital level. Dynamic balance was performed with checks of roll and pitch natural frequencies.



Figure 6. Scale model of the *World Utility* with remote control operation

Inertial Navigation System: The wave-induced oscillatory motions of the model *World Utility* ship were measured in the lab using an inertial navigation system (INS). An INS consists of accelerometers and angular rate sensors that measure the accelerations and angular rates in three directions and convert them to the six DOF motions (surge, sway, heave, roll, pitch, and yaw). A state-of-the-art INS system was obtained which could provide the high resolution required for small laboratory measurements. Details of this motion analysis system (MOTAN) can be found in Briggs and Sargent (2000) “Evaluate and acquire inertial navigation system

(INS),” Unpublished Technical Note, U.S. Army Engineer Research and Development Center, Vicksburg, MS.

The MOTAN system was installed on the scaled *World Utility* vessel near the CG of the model ship (Figure 7). The MOTAN Model 301 system (Miles and Pelletier 2000) was used, consisting of a BEI MotionPak inertial motion sensor unit, a data acquisition system, a battery power unit, and postprocessing software. The accuracy of the BEI MotionPak is 0.8 mm for data over a minimum duration of 10 (regular waves) to 15 (irregular waves) times the encounter period. Low and high frequency limits for data analysis are critical for accurate analysis. The low frequency limit is required to prevent spurious low frequency motions due to sensor noise. The high frequency limit is necessary to control high frequency noise in the computed accelerations that depend on the derivatives of the measured angular rate signals. Values of 3 and 25 sec (prototype scale) were used for these limits since they represent limiting wind wave periods for wave-induced ship motions. The data acquisition system uses a data logger to record the analog voltage signals from the six sensors. A sampling rate of 50 Hz was used to prevent aliasing of high frequency noise since there are no input filters and the natural frequency of the rate sensors is in the range of 15-20 Hz. Time synchronization with the wave-surface elevation data was performed daily to insure accurate comparisons. The MOTAN6 program computes displacement, velocity, and acceleration for each of the 6 DOF responses at specified points on the ship model.



Figure 7. MOTAN motion analysis system installed in the model ship

Wave Conditions: Seven wave gages (Figure 8) were positioned in the model to obtain significant wave heights. Four were located outside the channel and three were located on the channel center line. One gage was used to calibrate the deepwater wave conditions at the 30-m (100-ft) contour, and Gage 4 in the channel was positioned at the same relative location as the field pressure gage at Sta 2200. Table 3 lists the gage x/y coordinates and water depth. The

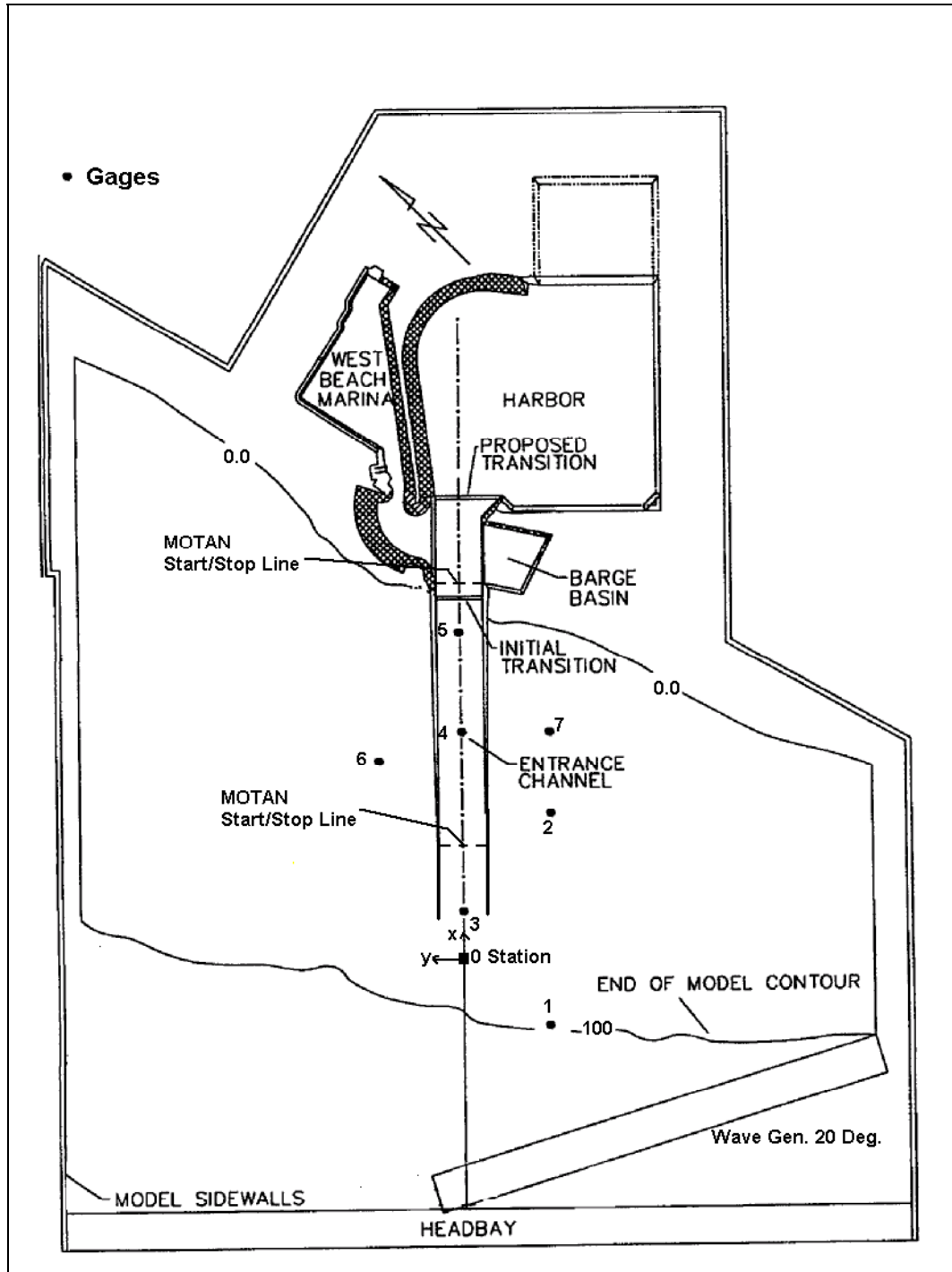


Figure 8. Schematic of Barbers Point Harbor physical model

right-hand coordinate system origin is at the channel Sta 0.0, with positive x-axis pointing toward the harbor and positive y-axis toward the west.

**Table 3
Gages Coordinates and Water Depths Barbers Point Harbor, HI**

Gage	Name	Coordinates, m		Water Depth, m
		X	Y	
W1	Incident-Toe	-166.2	-262.9	30.5
W2	Incident-East	391.8	-262.9	8.2
W3	Channel CL	96.7	0.0	12.8
W4	Channel CL	654.7	0.0	12.8
W5	Channel CL	894.3	0.0	12.8
W6	Incident-West	478.2	269.7	8.2
W7	Incident-East	654.7	-262.9	5.7

Notes:
1. Right-handed coordinate origin at channel Sta 0.00 and channel center line
2. Positive x-axis points toward harbor and positive y-axis toward west

Wave conditions were simulated in the laboratory based on the measured pressure gage data in the channel. Although waves from the south (i.e., 205 deg) and west (i.e., 260 deg) were tested, only the southerly waves are reported here since most of the observed directions during the field measurements were for waves from the south. Most of the ship transits occurred between the 3-hr measurement times of the channel pressure gage. Therefore, to properly bracket all possible wave conditions during the ship transit, the pressure gage data at the beginning and ending of this 3-hr interval were both simulated. Thus, two wave conditions were created for each inbound and outbound transit for each of the different ships. Because of pressure response factor and signal to noise considerations, it was not possible to estimate the field wave conditions beyond a 0.23-Hz (2-Hz laboratory) cutoff. Waves for one of the ships, the *Igrim*, were not considered in lab tests because this vessel is much smaller than the model ship used in the tests. Based on the buoy data, it was decided to use the 19 May case for the missing 30 May transit pressure gage data because the wave heights were similar.

Table 4 lists target and measured peak wave period T_p and significant wave height H_{m0} for these wave conditions at Gage 4. Figure 9 shows target and measured laboratory spectra for the sea-dominant DDU422 wave case, corresponding to the outbound WU transit on 30 May 99. Most of the target wave conditions were multimodal because of wave transformation in the entrance channel due to wave shoaling, breaking, refraction, and diffraction. In many cases the energy in these multiple peaks were nearly equal to each other. It was not possible to exactly reproduce the slight variations in energy for every peak or mode. In some cases, the largest peak in the measured spectrum was shifted from a sea to a swell peak, or vice versa. Although the difference in measured T_p then appears to be large (in two cases DDU122 and DDU622), the measured spectral shape actually matches the target spectrum reasonably well. Differences in measured H_{m0} are usually due to the inclusion of energy in the high frequency range in the laboratory spectrum between 0.23 to 0.35 Hz (the field measurements were cut off at 0.23 Hz). Because ship motions are not significantly affected by high frequency energy, it was not necessary to correct the control signals any further.

Table 4 Summary of Wave Parameters Barbers Point Harbor, HI								
Ship	Date	In / Out	Draft, m	Target for Gage 4			Measured at Gage 4	
				Signal	Hm0, m	Tp, sec	Hm0, m	Tp, sec
<i>Atoyac</i>	21-May	IN	9.52	DDU612	0.40	6.4	0.53	4.0
				DDU622	0.39	15.1	0.53	4.1
<i>Atoyac</i>	25-May	OUT	5.61	DDU712	0.32	9.5	0.30	9.6
				DDU722	0.30	5.3	0.30	5.4
<i>Carla A. Hills</i>	18-May	IN	6.01	DDU312	0.54	6.2	0.45	6.1
				DDU322	0.46	6.4	0.45	6.4
<i>Carla A. Hills</i>	19-May	OUT	8.18	DDU412	0.58	6.6	0.75	5.4
				DDU422	0.58	6.7	0.65	6.8
<i>Port Catherine</i>	14-May	IN	9.70	DDU112	0.43	5.4	0.38	5.5
				DDU122	0.47	17.1	0.53	5.4
<i>Port Catherine</i>	16-May	OUT	6.63	DDU212	0.42	12.8	0.45	12.2
<i>World Utility</i>	20-May	IN	5.36	DDU512	0.41	6.0	0.45	6.0
				DDU522	0.43	5.7	0.45	5.7
<i>World Utility</i>	30-May	OUT	10.84	DDU412	0.58	6.6	0.75	5.4
				DDU422	0.58	6.7	0.65	6.8

Testing Procedure: For each wave case, two runs (i.e., one repeat) were made for each inbound and outbound transit at two different vessel speeds and ship drafts. A slow and fast vessel speed was selected to bracket the range of possible ship speeds for inbound and outbound transits for all the ships. These speeds were calibrated with a series of speed trials. A quadratic, least squares fit was calculated to predict the ship speed as a function of the tachometer setting on the remote control. The assumption made was that the ship track was straight for all runs. A light ship and a fully-loaded draft were tested for each ship transit. Typically, eight runs (i.e., 2 runs x 2 speeds x 2 transits) were made for each wave condition and ship draft.

Inshore and offshore start/stop lines were located across the entrance channel for measuring ship motions using the MOTAN system. The inshore start/stop line was located near the shoreline at Sta 3430 and the offshore line near Sta 610. The beginning and ending times for each transit were recorded as the model ship crossed these start/stop lines. For inbound transits, the ship's stern was used as the reference to insure that the ship was completely within the flat part of the entrance channel. Similarly, for the outbound transits, the ship bow was used. The ship speed was also calculated by dividing the distance between these start/stop lines (858.4 m prototype units) by the travel time since the vessel speed was nearly constant during each transit. The two different methods of calculating ship speed were compared and the latter method was selected as the most accurate.

06 November 2001 11:36

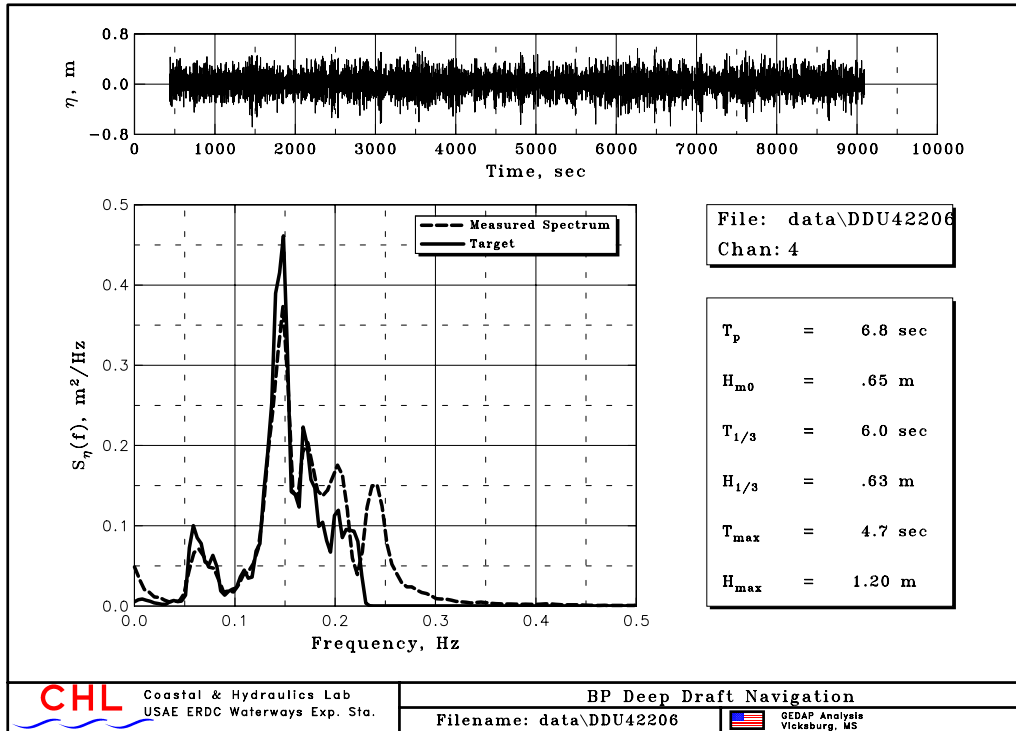


Figure 9. Target and laboratory wave case DDU422 for $T_p = 6.7$ sec and $H_{m0} = 0.58$ m

FIELD AND LABORATORY WAVE-INDUCED VERTICAL MOTIONS

Time Series of Wave-Induced Vertical Motions: Time series of the wave-induced vertical motions at the ship's CG as a function of channel location x ($h_{WA,CG}(x)$) were measured for each field transit and calculated for the laboratory runs. Figure 10 shows field and laboratory $h_{WA,CG}(x)$ for the outbound run of the fully-loaded *World Utility* from the harbor Sta 3800 to the offshore Sta 0. The blue line is the field measurements and the red line is the corresponding laboratory data. The match is very good. The difference in phasing between the two time series is insignificant as each is only one realization of an infinite ensemble of possible outcomes because of the randomness of ocean waves. The important consideration is that both field and laboratory values are the same order of magnitude and show the same trends within the entrance channel.

The measured ship speed v_{ship} for the field data is also shown on the right-hand side of this plot. It increases from a little over 4 knots to 6 knots as the ship leaves the entrance channel. The v_{ship} for the model run was constant at about 4.2 knots. The depth-related Froude numbers F_{nh} (i.e., $v_{ship}/(gh)^{0.5}$) for this range of ship speeds are in the subcritical range. Values are between $0.18 \leq F_{nh} \leq 0.28$ for $v_{ship} = 4$ knots and 6 knots, respectively. The dimensionless F_{nh} is often used in lieu of v_{ship} to describe ship motions.

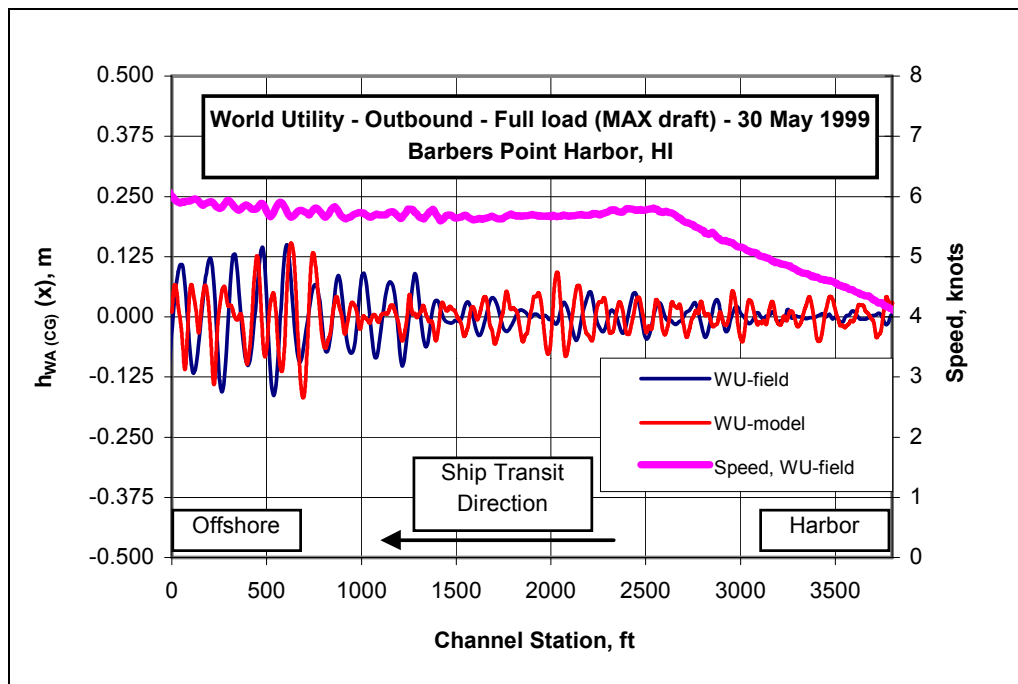


Figure 10. Measured field and laboratory $h_{WA,CG}(x)$ time series and field ship speed for the outbound *World Utility* with full load (MAX draft)

Maximum Wave-Induced Vertical Motion: The maximum value ($h_{WA,CG}$) of the $h_{WA,CG}(x)$ time series for each of the eight field runs (i.e., four ships, inbound and outbound transits, minimum and maximum drafts) is plotted versus channel station in Figure 11. This $h_{WA,CG}$ value was selected as the largest wave-induced motion (i.e., largest negative value) from each of the time series, with respect to the dockside static survey. The blue symbols represent the inbound vessels and the red symbols the outbound vessels. For the data in Figure 10, the $h_{WA,CG}$ for the field run is 0.17 m (0.55 ft) and occurs at channel Sta 550. The corresponding laboratory maximum is slightly larger and occurs near Sta 700. The agreement is very good. Since waves are largest at the offshore end of the channel, one would expect that the largest $h_{WA,CG}$ would occur here. This figure shows that large values of $h_{WA,CG}$ can occur along the entire length of the channel except near the shoreline where they have been reduced by wave transformation.

The comparison in Figure 10 is for just one of the laboratory runs for the outbound, fully-loaded *World Utility*. How do the other six outbound runs for the two laboratory wave conditions (one was lost due to low battery conditions) compare to the field value? Figure 12 shows the variation of $h_{WA,CG}$ for these cases for the two laboratory wave conditions (i.e., DDU412 and DDU422) as a function of ship speed. Ship speed was used in lieu of the nondimensional F_{th} because it is simpler to work with. The field measurement (i.e., the large closed circle) is shown for reference. The match between the laboratory and field cases is very good. The slow-speed cases are affected by the waves more than the high-speed cases since their $h_{WA,CG}$ values are larger. A linear least squares fit of $h_{WA,CG}$ versus ship speed for these seven laboratory data has a correlation coefficient of $R^2=0.71$. The predicted $h_{WA,CG}$ at the field ship speed is 0.13 m, underpredicting the measured $h_{WA,CG} = 0.17$ m by 25 percent.

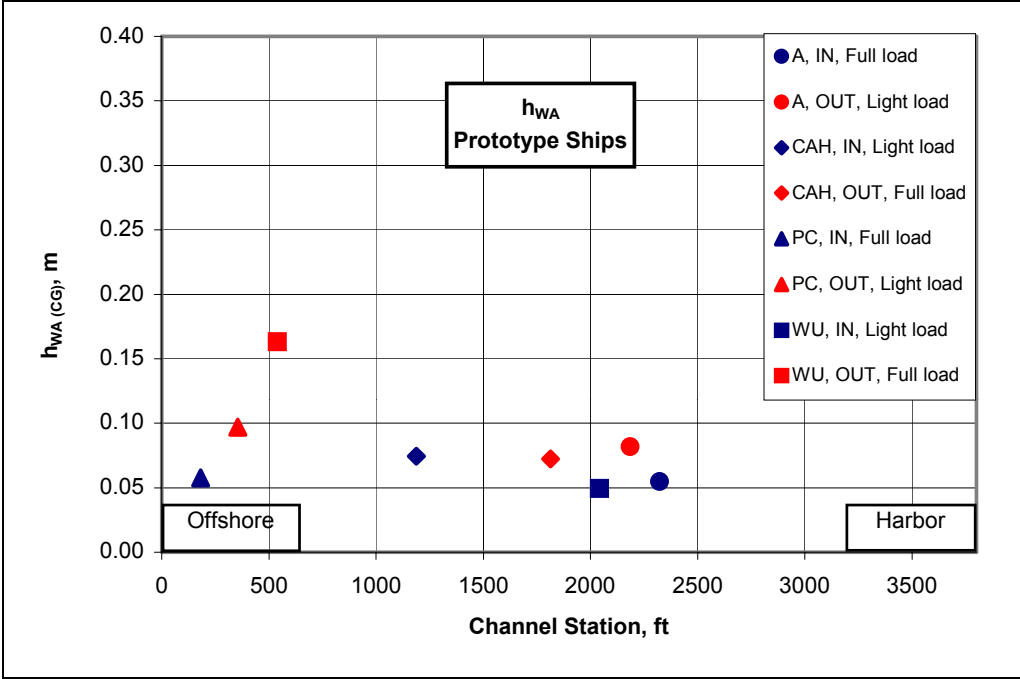


Figure 11. Maximum h_{WA,CG} for the four prototype ships

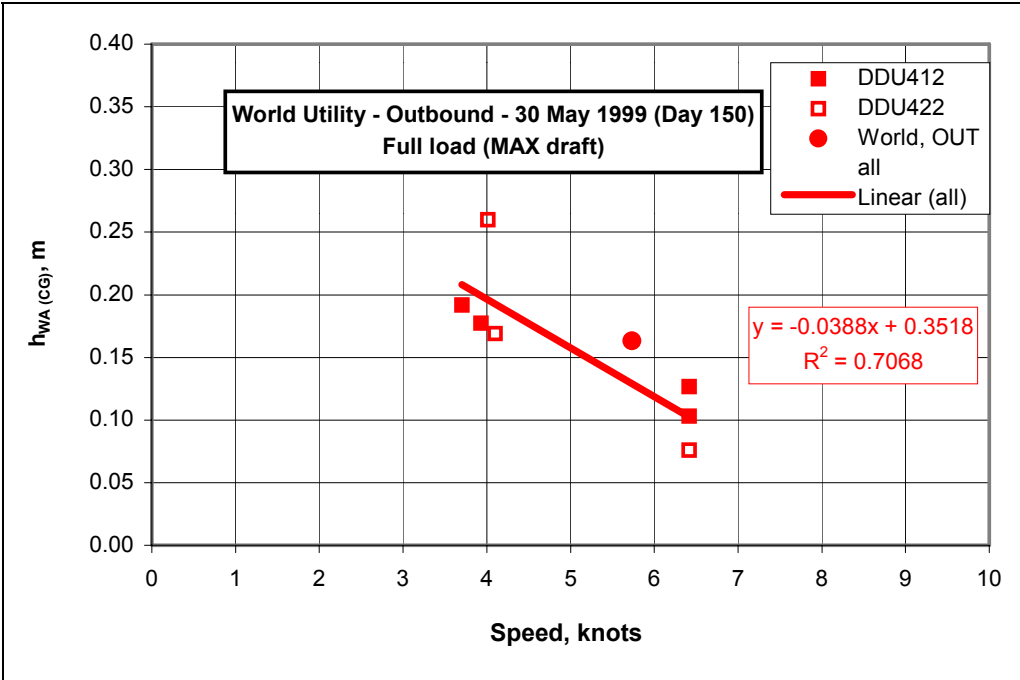


Figure 12. Comparison of field and laboratory h_{WA,CG} for the outbound World Utility with full load (MAX draft)

Four of the field vessels had similar sizes and shapes, even though two were tankers. Therefore, it is reasonable to compare the laboratory WU $h_{WA,CG}$ obtained for the range of wave conditions to the three other field $h_{WA,CG}$ values. Figure 13 shows the variation of the $h_{WA,CG}$ versus ship speed for all the laboratory and field runs for southerly waves (i.e., 205 deg). Only fully-loaded cases are included, with inbound runs in blue and outbound runs in red. Field values are shown with larger symbols to improve readability. The $h_{WA,CG}$ from the other field ships are smaller than the *World Utility* outbound run. They are, however, within the envelope of values measured in the laboratory. In general, the laboratory $h_{WA,CG}$ are two to three times larger than the field values. The magnitude of these differences is still very small, however.

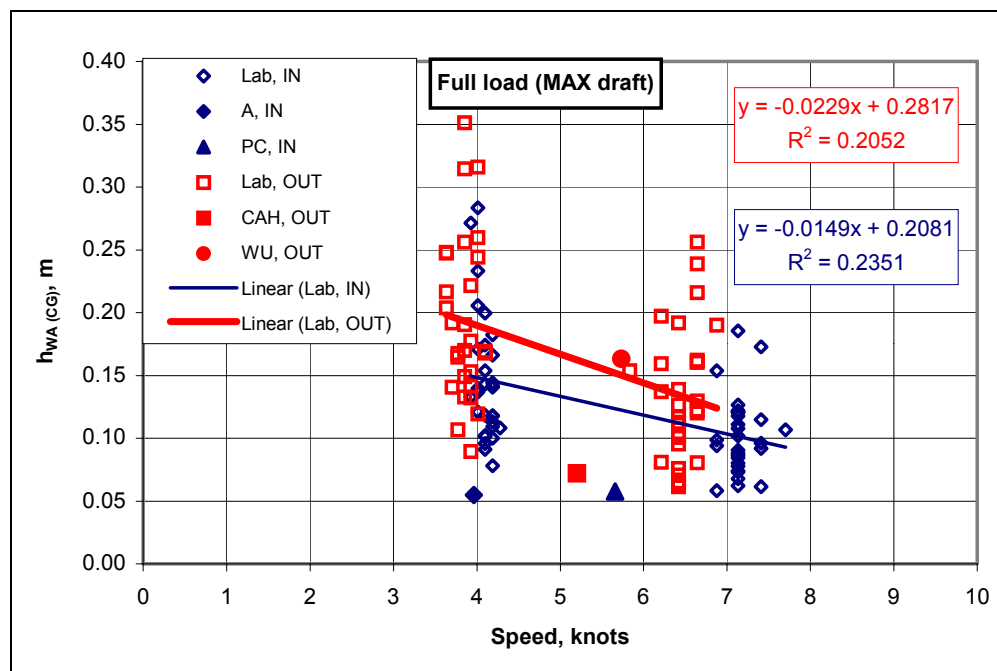


Figure 13. Comparison of all field and laboratory $h_{WA,CG}$ for ships with full load (MAX draft). Least squares linear fits for inbound and outbound ship transits are also shown

A linear least squares fit of the laboratory data is shown for both the inbound and outbound runs. Although the R^2 is very small for both inbound and outbound transits, it is very encouraging that the magnitudes are of the same order and the differences are very small. The laboratory outbound fit-line for $h_{WA,CG}$ lies between the two field points. The least squares fit for $h_{WA,CG} = 0.15$ is now closer to the largest measured $h_{WA,CG} = 0.17$ m from Figure 12. The predicted value is now only 12 percent smaller than the measured field value for the outbound *World Utility*. There are, however, many laboratory values that are larger than the measured field value. The laboratory inbound fit-line for $h_{WA,CG}$ lies above the field points. Thus, except for this one point, the laboratory data can be considered a conservative predictor of $h_{WA,CG}$, as they are all larger than the field values.

A possible explanation for some of this difference is the effect of directional spreading. The field data were obtained in a directionally-spread wave environment, whereas the laboratory data

waves were all unidirectional. Unidirectional waves were used because wave transformation processes would be more important in the entrance channel than wave directionality. Since it is a well-known fact that ships respond differently in a directionally-spread wave environment, it would be a reasonable next step to examine the effect of directional spreading with a multidirectional wavemaker.

Laboratory Scale Effects: One of the goals of these laboratory experiments was to demonstrate that laboratory scale effects do not significantly impact the measured results. The wave forcing for the Barbers Point data set was small, with prototype wave heights in the channel in the range of 0.30 to 0.58 m. One would not expect large ships like the *World Utility* to respond much to such a small wave height. Indeed, this was the case as the field measurements indicated vertical motions at the CG in the range of $h_{WA,CG} = 0.05$ to 0.17 m. These measurements correspond to a maximum vertical response of 30 percent (i.e., 0.17 m/0.58 m) of the wave height.

The worst case for the laboratory data was an underprediction of 25 percent for the outbound fully-loaded *World Utility* transit. When compared to the larger laboratory dataset for all the outbound fully-loaded transits, the underprediction was reduced to only 12 percent. Many of the laboratory values of $h_{WA,CG}$ were actually larger than the field values. In general, the laboratory is a conservative predictor of the maximum vertical motion as they are all larger than the corresponding field values.

The fact that the laboratory values were within an order of magnitude of the field values for such small wave heights is fairly remarkable. Most of the time ships experience larger wave heights, up to their design limits, during transits in entrance channels. The prototype wave heights measured at Barbers Point were smaller than the maximum possible values. Larger wave heights in the laboratory will only reduce any possible laboratory scale effects due to signal to noise or measurement tolerances. Thus, considerable confidence can be placed in this system as a tool for accurately measuring and predicting ship vertical motions.

SIGNIFICANCE TO UNDERKEEL CLEARANCE: The field data are based on an average from the three GPS sensors at approximately the vessel CG. All of the comparisons so far have been for wave-induced vertical motions at the CG. The CG does not experience as much vertical motion as other locations on the ship because it does not incorporate the wave-induced, vertical motions due to pitch and roll. Ship locations such as the bow and stern, and the forward and aft port and starboard sides experience the most h_{WA} . When calculating ships underkeel clearance h_{UKC} , these locations where the larger values of vertical motion occur should be used. Presently, we have software to calculate h_{WA} at these other locations only for the model ship (plans are to develop this capability for the field data). As an example, the $h_{WA,Bow}$ at the ship's bow for the laboratory data from Figure 12 was calculated and is shown in Figure 14. In general, the $h_{WA,Bow}$ are approximately three times larger than the corresponding $h_{WA,CG}$ values and exhibit the same trend. Thus, there is a significant difference between the wave-induced motion at the CG and the bow.

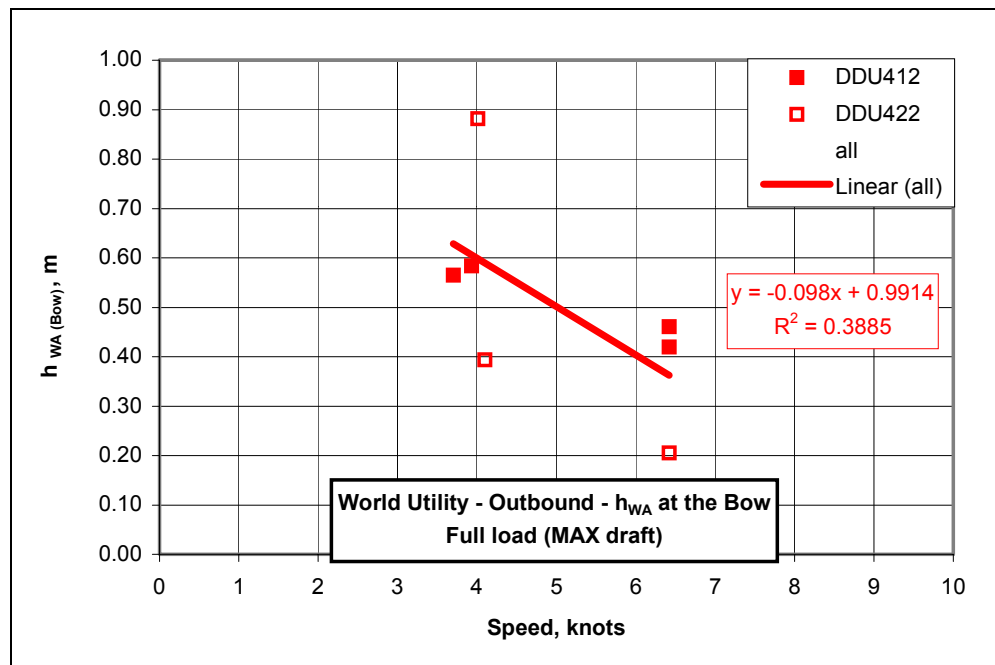


Figure 14. Calculated $h_{WA,Bow}$ at the *World Utility* for outbound runs with full load (MAX draft). A linear least squares fit is also shown

Example: How does the $h_{WA,Bow}$ at the ship's bow compare to the underkeel clearance h_{UKC} for the entrance channel? The purpose of this example is not to provide design guidance based on very limited laboratory data, but rather to show the relationship between the $h_{WA,Bow}$ and h_{UKC} for this data. This example does show, however, that the laboratory data give reasonable values for h_{UKC} .

The channel design depth h_{DC} is related to the fully-loaded ship draft T and h_{UKC} by

$$h_{DC} = T + h_{UKC} \quad (1)$$

Rearranging Equation 1 and inserting the existing Barbers Point $h_{DC} = 12.8$ m and $T = 10.9$ m for the *World Utility*, the maximum available h_{UKC} is only 1.9 m (6.2 ft). This is the maximum distance between the ship's keel and the seabed for the ships using Barbers Point at this time.

The next step is to compare this maximum available h_{UKC} to the h_{UKC} from the allowances. As stated previously, the h_{UKC} is composed of the four allowances

$$h_{UKC} = h_{WA} - h_{TI} + h_{SQ} + h_{SF} \quad (2)$$

where,

- h_{WA} = wave-induced motion allowance,
- h_{TI} = tide allowance,
- h_{SQ} = squat allowance, and

h_{SF} = safety factor allowance for bottom type.

From Figure 14, values of $h_{WA,Bow}$ range from 0.20 to 0.88 m. The worst-case h_{WA} occurred for the slow-speed case at $h_{WA,Bow} = 0.88$ m (2.9 ft). Most of the ship transits occurred on flood tide cycles, so the effective channel depth increased for these runs up to 0.7 m (2.3 ft). In the case of ebb tides, however, the channel depth would need to be reduced. The actual tide during the outbound *World Utility* run on May 30, 1999 was $h_{TI} = + 0.20$ m (0.66 ft). Squat was not measured in either the field or laboratory measurements. Field measurements from the low pass filtering of the data (see "Prototype Measurements" section) indicated that it was of the order of 0.3 m (1 ft). Several empirical estimates of squat were presented in Demirbilek and Sargent (1999). In general, it depends on the vessel speed and the channel blockage, which is a ratio of the ship cross-sectional area to the channel area. According to Figures 5-3 and 6-4 in EM 1110-2-1613 (HQUSACE 1995) for a trench-type channel like Barbers Point, h_{SQ} should be of the order of 0.2 to 0.3 m (0.66 to 1.0 ft) for ship speeds during the field measurements. Finally, the h_{SF} accounts for the type of seabed. For hard bottoms (as at Barbers Point), an $h_{SF} = 0.91$ m (3 ft) is recommended.

Inserting these values for the allowances into Equation 2 for the worst-case h_{UKC} that occurred for the slow-speed case on flood tide

$$h_{UKC} = 0.88 - 0.20 + 0.20 + 0.91 = 1.79 \text{ m} \quad (3)$$

Comparing this value to the maximum h_{UKC} at Barbers Point from Equation 1, there is only a reserve of 0.11 m (i.e., 1.90 m - 1.79 m) (0.36 ft) in underkeel clearance available for use for larger waves and low tides. No advance maintenance or dredging tolerance allowance h_{AM} was included, but because there is generally no silting problem due to the hard coral bottom, this is probably not necessary at Barbers Point. There is some clearance in the h_{SF} that can be used for larger wave heights, so the existing channel depth is adequate. Based on this analysis with a very limited data set, it does not appear that the existing channel depth is overly conservative.

How does the measured h_{WA} compare to the existing guidance? Again, the point is to show that the laboratory data are reasonable relative to existing guidance. Additional data for a variety of ships and wave and channel conditions will be needed to make a recommendation in channel design guidance. EM 1110-2-1613 recommends $h_{WA} = \alpha H_I$, where $\alpha = 1.2$. Figure 15 shows the normalized ratio $\alpha_{meas} = h_{WA}/H_I$ for the laboratory data of Figure 14. The larger laboratory values of $H_I = 0.75$ m and 0.65 m for the DDU412 and DDU422, respectively, were used rather than the field value of $H_I = 0.58$ m. Thus, the α_{meas} ranges from a minimum of 0.3 to 1.3. The EM 1110-2-1613 guidance is based on an assumed maximum value of pitch and roll angles in a static environment without dynamic effects from the waves in combination. Thus, the h_{WA} are smaller than the guidance, except for the case of $\alpha_{meas} = 1.3$.

The PIANC (1997) recommends $\beta T \leq h_{WA} \leq 2\beta T$, where $\beta = 0.2$. The smaller value is for wave heights less than 1 m. For the model ship draft $T = 10.9$ m, the corresponding values are $2.2 \text{ m} \leq h_{WA} \leq 4.4 \text{ m}$. These values are two and a half to five times larger (i.e., $2.2/0.88 = 2.5$) than the measured h_{WA} largest value. Finally, the measured β_{meas} can be obtained by dividing the measured h_{WA} by T . The range of values for β_{meas} varied between $0.02 \leq \beta_{meas} \leq 0.08$, a

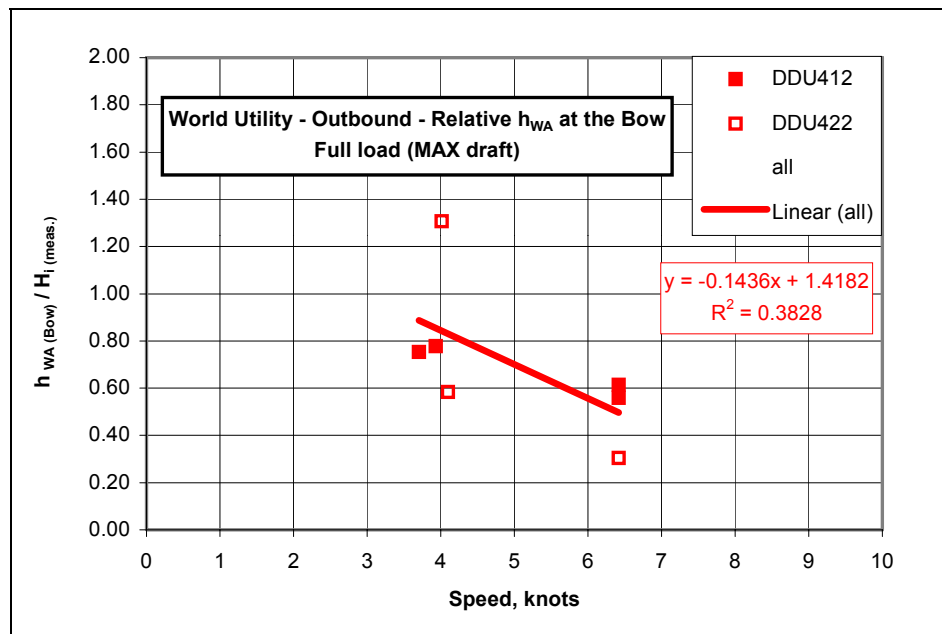


Figure 15. Normalized $h_{WA,Bow}$ for the *World Utility* for outbound runs with full load (MAX draft). A linear least squares fit is also shown

difference of 2.5 to 10 times the PIANC value of $\beta = 0.2$. The β_{meas} are much smaller than the PIANC guidance. Future analysis will include the results from the other laboratory data in these comparisons.

SUMMARY: This Technical Note summarizes preliminary comparisons between field and laboratory measurements of wave-induced vertical motions at Barbers Point Harbor. Prototype ship motions and environmental data were obtained in May 1999 for five ships. These field measurements were reproduced in a controlled laboratory study with a model of the *World Utility*, typical of the ships studied. In this laboratory procedure, it was determined that scale effects were not significant. Preliminary comparisons between laboratory and field measurements were very encouraging and provide confidence in the ability to accurately replicate and measure complicated ship motion responses in the laboratory. These results show that laboratory models are capable of predicting slightly conservative estimates of wave-induced vertical motions for a range of wave conditions. An example was provided to illustrate the relationship between the wave-induced, vertical ship motions and underkeel clearance.

This was a very limited data set based on one entrance channel, one ship, and one draft. Maximum wave-induced vertical motions at several other locations on the model ship can be compared to the $h_{WA,Bow}$ value. Typically, the bow location experiences the largest vertical motion, but other locations along the ship's keel should be investigated. Additional data are being compared for the light ship condition of the *World Utility* vessel. Although these data are less interesting from the channel draft perspective, it is a useful data set for comparing ship response under different loading conditions. Prototype data were also collected for different ships and entrance conditions at Charleston Harbor, SC. Future plans include additional laboratory verification with these data.

Additional work is ongoing in several areas to improve this data set. First, we will examine the error inherent in comparing field $h_{WA,CG}$ at a point that does not correspond exactly to the ship CG. This small variation in the location of the field average $h_{WA,CG}$ might explain some of the observed variation between laboratory and field. Second, response amplitude operators (RAO) are being calculated for each transit that will show the vessel response as a function of the wave conditions. These RAO's can then be used to predict the ship's six DOF motions for different wave conditions and spectral shapes. Third, the effect of wave directionality needs to be quantified. The laboratory waves were simulated with a unidirectional wavemaker, even though the field waves did exhibit some spreading. Additional testing with multidirectional waves would be required. Finally, we are working to analyze the laboratory data in a probabilistic sense that will make it more useful for predicting h_{WA} for other wave conditions and ship types. The random nature of waves can be incorporated in the prediction algorithm to include some uncertainty.

Squat is an integral part of the underkeel clearance. Unfortunately, it is not possible to measure it in the laboratory with the MOTAN system. Upgrades to our existing set of infrared Charged Coupled Device (CCD) cameras would be required to provide the extreme level of accuracy required to measure squat. These cameras have the added advantage that they can show ship tracks in the channel during transits. The combination of these two systems would provide a state-of-the-art capability for measuring ship motions in the laboratory.

The goal of this research is to develop data to support improvements to the ERDC ship simulator and provide an empirical approach to aid in coastal entrance channel design. This will minimize project and maintenance dredging costs and allow quick assessment of proposed changes in channel design. Field measurements are preferred, but are expensive to obtain and have the risks inherent in field data collection. A verified physical model is less expensive and provides a more controlled environment for generating empirical data for a range of channel, ship, and wave conditions. These results give us confidence that laboratory models can be used as an effective tool in optimizing entrance channel depths, as well as developing empirical data sets needed to support other research and development needs.

ADDITIONAL INFORMATION: For additional information, contact Dr. Michael J. Briggs (Voice: (601) 634-2005, e-mail: Michael.J.Briggs@erdc.usace.army.mil) or Dr. Zeki Demirbilek (Voice: (601) 634-2834, e-mail: Zeki.Demirbilek@erdc.usace.army.mil). This Technical Note should be cited as follows:

Briggs, M., Melito, I., Demirbilek, Z., and Sargent, F. (2001). "Deep-draft entrance channels: Preliminary comparisons between field and laboratory measurements," Coastal and Hydraulics Engineering Technical Note CHETN-IX-7, U.S. Army Engineer Research and Development Center, Vicksburg, MS.
<http://chl.wes.army.mil/library/publications/chetn/>

REFERENCES

- Borgman, L. E. (2001). "Report on visit to CHL, August, 2001 and the review of programs," Contract DAC42-01-P-0340, L.E. Borgman, Inc., Vicksburg, MS.
- Briggs, M. J., Lillycrop, L. S., Harkins, G. S., Thompson, E. F., and Green, D. R. (1994). "Physical and numerical model studies of Barbers Point Harbor, Oahu, Hawaii," Technical Report CERC-94-14, U.S. Army Engineer Waterways Experiment Station, Vicksburg, MS.
- Demirbilek, Z., and Sargent, F. (1999). "Deep-draft coastal navigation entrance channel practice," Coastal Engineering Technical Note CETN-I-63, U.S. Army Engineer Research and Development Center, Vicksburg, MS.
- Harkins, G. S., and Dorrell, C. C. (2000). "Barbers Point Harbor physical model navigation study," U.S. Army Engineer Research and Development Center, Vicksburg, MS.
- Headquarters, U.S. Army Corps of Engineers. (1995). "Hydraulic design guidance for deep-draft navigation projects," Engineer Manual 1110-2-1613, Washington, DC.
- Miles, M. D., and Pelletier, D. (2000). "User's guide and reference manual for the MOTAN model 301 inertial motion measurement system," Technical Report HYD-CTR-085, Canadian Hydraulics Center, Ottawa, Ontario, Canada.
- Permanent International Association of Navigation Congresses (PIANC). (1997). "Approach channels: A guide for design," Supplement No. 95.